The miR-144/451 locus is required for erythroid homeostasis

Kasper D. Rasmussen,[1] Salvatore Simmini,[1] Cei Abreu-Goodger,[2] Nenad Bartonicek,[2] Monica Di Giacomo,[1] Daniel Bilbao-Cortes,[1] Rastislav Horos,[3] Marieke Von Lindern,[3] Anton J. Enright,[2] and Dónal O'Carroll[1]

[1]European Molecular Biology Laboratory, Mouse Biology Unit, Monterotondo Scalo, 00015, Italy
[2]European Bioinformatics Institute, Hinxton, Cambridge, CB10 1SD, UK
[3]Department of Hematology, Erasmus MC, 3015 GE Rotterdam, Netherlands

The process of erythropoiesis must be efficient and robust to supply the organism with red bloods cells both under condition of homeostasis and stress. The microRNA (miRNA) pathway was recently shown to regulate erythroid development. Here, we show that expression of the locus encoding miR-144 and miR-451 is strictly dependent on Argonaute 2 and is required for erythroid homeostasis. Mice deficient for the miR-144/451 cluster display a cell autonomous impairment of late erythroblast maturation, resulting in erythroid hyperplasia, splenomegaly, and a mild anemia. Analysis of gene expression profiles from wild-type and miR-144/451–deficient erythroblasts revealed that the miR-144/451 cluster acts as a "tuner" of gene expression, influencing the expression of many genes. MiR-451 imparts a greater impact on target gene expression than miR-144. Accordingly, mice deficient in miR-451 alone exhibited a phenotype indistinguishable from miR-144/451–deficient mice. Thus, the miR-144/451 cluster tunes gene expression to impart a robustness to erythropoiesis that is critical under conditions of stress.

CORRESPONDENCE
Dónal O'Carroll:
ocarroll@embl.it

Abbreviations used: Ago, Argonaute; E, embryonic day; miRNA, microRNA; qRT-PCR, quantitative RT-PCR; RISC, RNA-induced silencing complex; TSS, transcription start site; UTR, untranslated region.

Erythrocytes are by far the most abundant cell type found in the blood, and their numbers in the periphery are tightly controlled. Much of the hematopoietic effort is directed at maintaining homeostasis of this relatively short-lived cell type. Astonishingly, the output of RBC production in humans under steady-state conditions is estimated to be about 2 million cells per second. Once committed to the erythroid lineage, precursors undergo numerous rounds of proliferation to amplify the pool of cells that will undergo terminal differentiation. The differentiation of erythroblasts to erythrocytes involves large morphological changes as the cells hemoglobinize, undergo dramatic size reduction, nuclear condensation, enucleation, and assume a discoid shape. This system has also evolved to cope with stress events such as traumatic blood loss, wherein the organism requires the efficient replenishment of a large volume of blood. Because of the constant demand for nascent RBCs under normal homeostasis, and especially in conditions of stress, the process of erythropoiesis must be both effective and robust (Broudy et al., 1996; Bauer et al., 1999).

Micro RNAs (miRNAs) are genome-encoded small noncoding RNAs that posttranscriptionally regulate gene expression, either through the inhibition of translation or degradation of target mRNAs (Bushati and Cohen, 2007). The miRNA-binding Argonaute (Ago) proteins are key components within the RNA-induced silencing complex (RISC) involved in biogenesis and execution of miRNA function (Hammond et al., 2001; Hutvágner and Zamore, 2002; O'Carroll et al., 2007). The RISC-bound miRNA base pairs with sites predominantly in the 3′ untranslated regions (UTRs) of mRNAs to confer target specificity. In animals, most miRNAs do not display perfect complementarity, and the specificity is primarily defined by the "seed" (bases 2–8) sequence of the miRNA (Doench and Sharp, 2004). It was recently shown that some miRNAs modestly repress hundreds of target transcripts within a

The Rockefeller University Press $30.00
J. Exp. Med. Vol. 207 No. 7 1351-1358
www.jem.org/cgi/doi/10.1084/jem.20100458

The Journal of Experimental Medicine

cell (Lim et al., 2005; Baek et al., 2008; Selbach et al., 2008), indicating that miRNAs not only function as developmental switches, but also as tuners of gene expression (Baek et al., 2008; Selbach et al., 2008).

RESULTS AND DISCUSSION

miR-144/451 expression in erythroblasts depends on Ago2

Recent studies revealed an essential role for Ago2 and the miRNA pathway during mammalian erythroid differentiation (O'Carroll et al., 2007). To identify miRNA loci that contribute to terminal erythropoiesis we used the following set of criteria: expression of the candidate miRNAs should be (a) down-regulated substantially in the absence of Ago2, (b) abundant in erythroblasts, and (c) restricted to the erythroid lineage. Expression profiling revealed that miR-451 was abundantly expressed, but completely absent in Ago2$^{-/-}$ erythroblasts (Fig. 1, A and B). This is in stark contrast to other miRNAs that were down-regulated but still expressed. The gene encoding miR-451 is located on chromosome 11, and encompasses a noncoding transcriptional unit that also encodes miR-144 that resides 5′ of miR-451 (Fig. S1 A). Mir-144 was also abundantly expressed in erythroblasts and markedly down-regulated in the absence of Ago2 (Fig. 1, A and B). Expression analysis of both miR-451 and miR-144 within lineage-restricted lymphocytes, granulocytes/monocytes, and erythroid cells revealed that the locus was selectively expressed within the erythroid lineage (Fig. 1 C; Lu et al., 2008). The expression of miR-451 was restricted to the fetal liver in embryonic day (E) 16.5 mouse embryos, the major site of hematopoiesis and erythropoiesis at this stage of

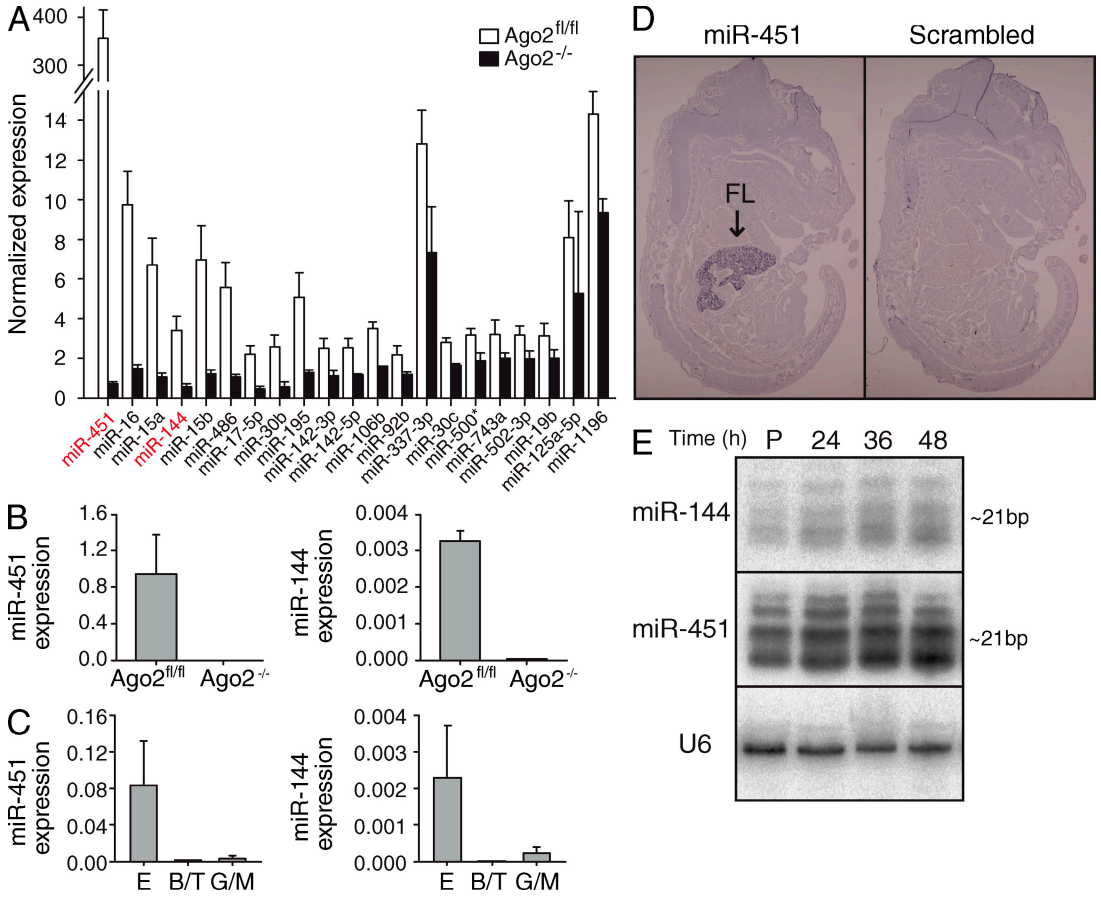

Figure 1. Expression of miR-144/451 locus is dependent on Ago2 and restricted to the erythroid lineage. (A) The levels of miRNA expression in sorted Ago2$^{fl/fl}$ and Ago2$^{-/-}$ erythroblasts (Ter119^{hi}CD71^{hi}) were measured by miRNA array profiling. Graph shows expression, normalized to the housekeeping genes RNU6A, RNU6B, SNORD2, and SNORD3A, of miRNAs displaying >1.5-fold down-regulation in Ago2$^{-/-}$ erythroblasts. The mean and standard deviation from three independent experiments are shown. (B) Expression of miR-451 and miR-144 in erythroblasts was quantified by qRT-PCR and graphs show expression normalized to U6 snRNA. The mean and standard deviation of two independent measurements are shown. (C) Expression of miR-144 and miR-451 quantified by qRT-PCR in erythroid (E), lymphoid (B/T), and granulocyte/monocyte cells (G/M). The mean and standard deviation of two independent measurements are shown. (D) The spatial expression of miR-451 is shown by in situ hybridization on saggital sections of E16.5 dpc mouse embryos; hybridization with a control scrambled probe is also shown. Arrow indicates miR-451 expression in the fetal liver (FL). Representative images from one of three independent experiments are shown. (E) The expression of miR-451 and miR-144 was measured by Northern blotting of RNA derived from a fetal liver culture under conditions that promote proliferation (P) or differentiation. Numbers show hours in differentiation conditions. U6 snRNA was used as a loading control. The Northern was performed once from a representative fetal liver culture.

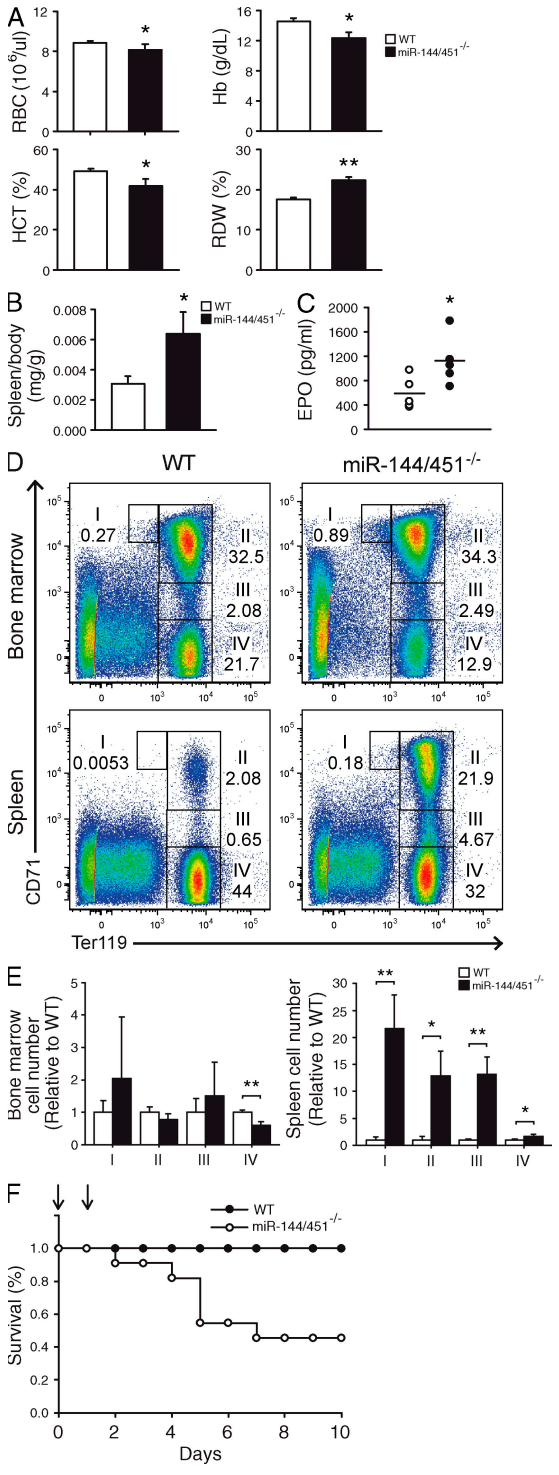

Figure 2. MiR-144/451 deficiency results in erythroid hyperplasia, ineffective erythropoiesis, and anemia. (A) MiR-144/451 deficiency alters several erythrocyte parameters in the peripheral blood. Bar graphs are shown expressing values for RBC, hemoglobin (Hb), hematocrit (HCT); and red cell distribution width (RDW). Bars represent mean values ($n = 5$), error bars indicate standard deviation. (B) Splenomegaly in miR-144/451$^{-/-}$ mice. Bars represent mean values ($n = 5$), error bars indicate standard deviation. (C) Erythropoietin (EPO) concentrations in plasma in miR-144/451$^{-/-}$ and wild-type littermate controls. The individual and mean EPO values are plotted for five independent measurements. (D) Representative FACS analysis of erythroid cell populations in the bone marrow and spleen of wild-type and miR-144/451$^{-/-}$ mice. Roman numerals and numbers indicate the identity and percentages of cells of the developmentally defined subpopulations (Socolovsky et al., 2001): I, proerythroblasts; II, basophilic erythroblasts; III, polychromatophilic erythroblasts; IV, orthochromatophilic erythroblasts. (E) Comparative enumeration of erythroid precursors in the bone marrow and spleen of miR-144/451$^{-/-}$ and wild-type mice. Numbers are expressed relative to the wild-type and plotted for the developmentally defined erythroid subpopulations indicated in D by roman numerals. The data in A, B, D, and E are representative of three independent experiments. (F) Survival plot of wild-type ($n = 11$) and miR-144/451$^{-/-}$ ($n = 11$) mice treated with phenylhydrazine. As indicated by the arrows, days 0 and 1 mark the days of the first and second injection, respectively. The data represent two independent experiments. *, $P < 0.05$; **, $P < 0.0001$.

development (Fig. 1 D). Furthermore, both miR-451 and miR-144 were expressed in fetal liver–derived erythroid cultures under media conditions that promote proliferation or terminal differentiation (Fig. 1 E). Indeed, consistent with our identification of miR-144/451 as putative miRNAs required for terminal erythropoiesis, the miR-144/451 locus was recently identified as a target gene of the essential erythroid transcription factor Gata1 (Dore et al., 2008).

MiR-144/451 deficiency results in erythroid hyperplasia, ineffective erythropoiesis, and a mild anemia

MiR-451 and miR-144 met all our criteria for miRNAs with a key function during mammalian terminal erythropoiesis; therefore, we proceeded to generate a mouse miR-144/451 cluster-null allele (miR-144/451^{-}) by *deleter*-Cre–mediated (Schwenk et al., 1995) excision of the loxP-flanked miR-144/451 allele (Fig. S1 B). MiR-144/451$^{-/-}$ mice were born in Mendelian numbers, survived throughout adulthood without increased rates of mortality, and showed no developmental defects in the lymphocyte or granulocyte-monocyte lineages (unpublished data). However, analysis of adult hematopoiesis in miR-144/451$^{-/-}$ mice revealed defects during terminal erythropoiesis. Peripheral blood showed a mild anemia with reduced red cell numbers and hematocrit and hemoglobin values, as well as increased red cell distribution width, indicating anisocytosis (Fig. 2 A and Fig. S2 A). The miR-144/451$^{-/-}$ mice also displayed splenomegaly, indicating compensation of anemia by stress erythropoiesis (Fig. 2 B). The anemia and stress erythropoiesis was confirmed by elevated erythropoietin concentrations (Fig. 2 C) and increased numbers of splenic c-kit–positive erythroid precursors in miR-144/451$^{-/-}$ mice (Fig. S2, B and C). Analysis of erythroid development revealed ineffective erythropoiesis in the bone marrow of miR-144/451$^{-/-}$ mice characterized by the normal presence of early basophilic erythroblasts (Ter119^{hi} CD71^{hi}), but a marked decrease in the frequency and number of mature orthochromatophilic (Ter119^{hi}, CD71^{neg}) erythroblasts (Fig. 2, D and E). In the mouse, inefficient erythropoiesis in the bone marrow can be compensated by stress erythropoiesis in the spleen

(Broudy et al., 1996; Bauer et al., 1999). Analysis of splenic erythroblast populations in miR-144/451$^{-/-}$ mice revealed an ~10-fold increase in the absolute numbers of early erythroblasts (Fig. 2 E), but normal or slightly elevated numbers of mature orthochromatophilic erythroblasts, indicating a major loss of cells during late erythroid maturation. Thus, miR144-451 deficiency impairs late erythroid differentiation, which is partly compensated by expansion of the early erythroid compartment in the spleen (Fig. 2, D and E, and Fig. S2 D). A function for miR-144/451 in both zebrafish and mouse erythropoiesis has been reported. However, data from zebrafish were conflicting as to the phenotypic consequences of miR-451 inhibition (Dore et al., 2008; Du et al., 2009; Pase et al., 2009). In the mouse, contrary to our observations, it was reported that inhibition of miR-144/451 impaired the proerythroblast to basophilic–erythroblast transition (Papapetrou et al., 2009). This discrepancy likely arises from the lentiviral decoy method of miRNA inhibition used.

The mild anemia in resting miR-144/451$^{-/-}$ mice may underrepresent the importance of the miR-144/451 locus to the hematopoietic homeostasis under situations of stress. We therefore challenged wild-type and miR-144/451$^{-/-}$ mice with phenylhydrazine, a chemical that induces hemolytic anemia, and assayed the potential of the mice to recover. Over half of the miR-144/451$^{-/-}$ mice died within 6 d after the administration of phenylhydrazine, whereas all wild-type littermates made a full recovery (Fig. 2 F). These results indicate that the miR-144/451 locus is critical for a robust hematopoietic system.

The defects in miR-144/451$^{-/-}$ mice are erythroid autonomous

Although unlikely, one could argue that the defects observed in the miR-144/451$^{-/-}$ mice are not hematopoietic autonomous and that they do not represent a developmental defect, but are a consequence of the response to a hemolytic anemia. The hematopoietic-intrinsic nature of the developmental defects in

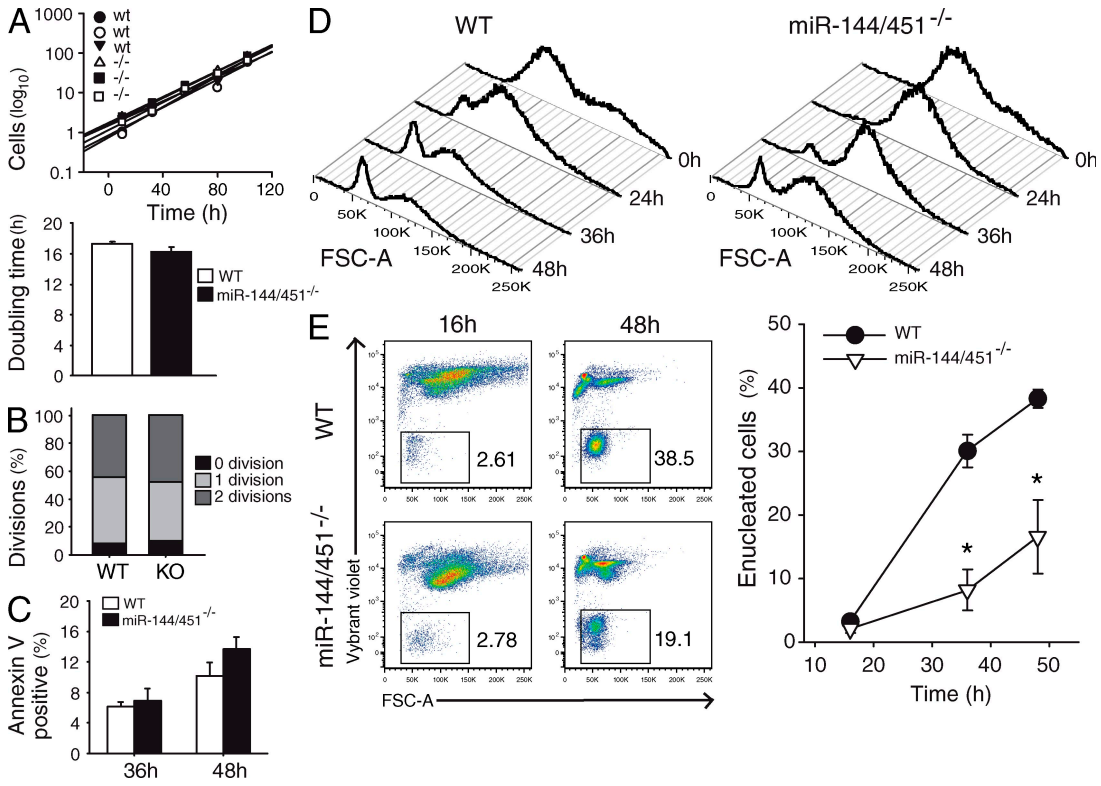

Figure 3. MiR-144/451 is intrinsically required for terminal erythroid differentiation. (A) Cumulative growth curve (top) and the respective calculated doubling times (bottom) for wild-type and miR-144/451$^{-/-}$ fetal liver cells. The data are from biological triplicates and representative of two independent experiments. (B) Stacked column plot shows the number of cell divisions of wild-type and miR-144/451$^{-/-}$ fetal liver cells 48 h after the induction of terminal differentiation as determined by CFSE labeling. The data are representative of one experiment using biological triplicates. (C) Bar graphs show apoptotic fetal liver cells defined by Annexin V positivity in wild-type ($n = 3$) and miR-144/451$^{-/-}$ ($n = 3$) erythroid cultures at the indicated time points. Data represent mean values, error bars indicate standard deviation. No statistical differences were observed. The data are representative of two independent experiments. (D) The size distribution (FSC-A) of live fetal liver cells at the indicated time points during in vitro terminal differentiation as determined by FACS is shown for wild-type and miR-144/451$^{-/-}$ cultures. Representative plots of four independent experiments are shown. Independent measurements for D are already mentined. (E) Representative FACS analysis of erythroid cell populations in the in vitro fetal liver cultures at the indicated times (left). The gated small Vybrant violet-negative cells represent nascent reticulocytes. The graph depicts the mean number of reticulocytes as determined by FACS in wild-type and miR-144/451$^{-/-}$ differentiation cultures at the indicated times (right). Points represent mean values ($n > 3$), error bars indicate standard deviation. The data in D and E are representative of three independent experiments. *, $P < 0.0001$.

miR-144/451$^{-/-}$ mice was revealed through the analysis of lethally irradiated mice reconstituted with miR-144/451$^{-/-}$ bone marrow. These reconstituted mice present the same defects as germline-deficient miR-144/451$^{-/-}$ mice (Fig. S3). We next used an in vitro fetal liver–derived erythroid cell culture and differentiation system (Dolznig et al., 2001; von Lindern et al., 2001) to investigate the intrinsic nature of the developmental defect. Fetal livers from wild-type and miR-144/451$^{-/-}$ E12.5 embryos were placed in culture with a cocktail of defined cytokines that promote the selective expansion of erythroid precursors. Under these conditions miR-144/451$^{-/-}$ erythroid precursors proliferated at the same rate as the respective wild-type controls (Fig. 3 A). After 3 d of expansion, the cultures were switched to differentiation medium. MiR-144/451$^{-/-}$ cultures normally underwent the final rounds of proliferation before entering terminal erythropoiesis (Fig. 3 B), as well as hemoglobinization (Fig. S2 E). In addition, no differences in the fraction of apoptotic cells were detected in the absence of miR-144/451 (Fig. 3 C). However, size reduction and enucleation of miR-144/451$^{-/-}$ cultures was inefficient (Fig. 3, D and E, and Fig. S2 E). MiR-144/451 deficiency did not block any one process, per se, but rendered terminal erythroid differentiation inefficient. Thus, the in vitro system recapitulated the defective erythropoiesis observed in vivo in miR-144/451$^{-/-}$ mice. These observations prove that the miR-144/451 cluster is not required for expansion of early erythroblasts, but is intrinsically required for terminal erythroid development.

The miR-144/451 locus tunes the expression of many genes

We next wanted to explore the extent and nature of the deregulated genes in the absence of miR-144/451 during terminal erythropoiesis. To this end, we decided to use the in vitro culture model, as it presented advantages over ex vivo isolated erythroblasts. The miR-144/451$^{-/-}$ erythroblasts in vivo are subjected to, among other things, altered cytokine levels and microenvironments. We detected a significant deregulation of gene expression in miR144/451$^{-/-}$ erythroblasts (Fig. 4 A). Transcriptome analysis from cells with either loss or gain of function for a given miRNA has been used to reliably identify miRNA targets because of transcript destabilization after RISC binding (Lim et al., 2005; Giraldez et al., 2006; Baek et al., 2008; Selbach et al., 2008; Lewis et al., 2009). To identify miR-144/451 target genes, we therefore used the Sylamer algorithm (van Dongen et al., 2008) to analyze the gene expression profiles derived from wild-type and miR-144/451$^{-/-}$ erythroid precursors. Sylamer searches for significant enrichment of 6-8 nt motifs across an ordered gene list. For miRNA analysis, the identification of miRNA seed match enrichment in the 3′ UTRs of deregulated genes from genome-wide experiments indicates direct miRNA involvement (van Dongen et al., 2008).

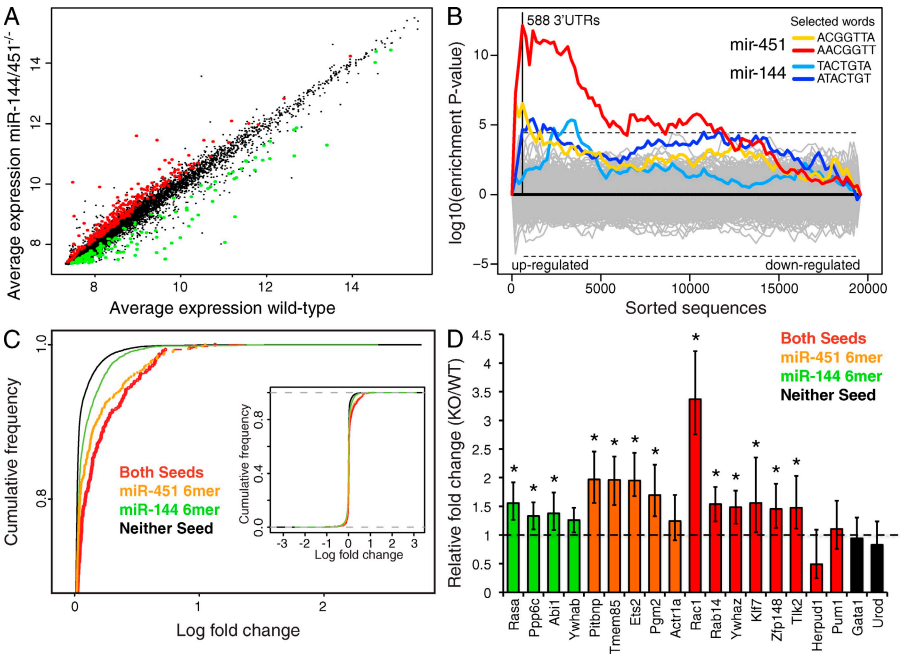

Figure 4. The miR-144/451 locus tunes the expression of many genes. (A) Expression scatterplot showing relative mean expression of Illumina probes in wild-type (x axis) and miR-144/451$^{-/-}$ (y axis) erythroblasts. Significantly up-regulated genes (red) and down-regulated genes (green) are shown. Expression profiling was performed once with biological quadruplicates of each genotype. (B) Sylamer enrichment landscape plot for all 876 7-nt motifs complementary to canonical mouse miRNA seed regions, either from nt 2–8 (7mer-m8) or from nt 1–7 (7mer-A1). The x axis represents the sorted gene list of 19,600 genes from most up-regulated to most down-regulated in the miR-144/451$^{-/-}$ erythroblasts. Each 7mer motif was tested for significant enrichment across the 3′ UTRs of genes in this list. The two motifs corresponding to seeds matching miR-451 (red, 7mer-m8; yellow, 7mer-A1) are enriched in the up-regulated genes, peaking at the most up-regulated 588 genes (solid vertical line). Two motifs matching the seed region of miR-144 (blue, 7mer-m8; light blue, 7mer-A1) are also significantly enriched, but to a lesser extent. The horizontal dotted lines represent a Bonferroni-corrected P value threshold of 0.05. (C) Upper region of an empirical cumulative density plot of log fold change for different populations of probes. Those probes whose 3′ UTRs possess miR-144 6-nt seed matches (green), miR-451 6-nt seeds (orange), or both seeds (red) are skewed toward higher positive fold changes in the miR-144/451$^{-/-}$ erythroblasts, compared with probes whose mapped 3′ UTRs do not contain a seed match (black). (D) qRT-PCR expression analysis of representative miR-144/451 seed-containing deregulated genes identified by Sylamer. Normalized data are plotted as relative fold change in miR-144/451$^{-/-}$ versus wild-type erythroblasts. Standard error is shown and * indicates significantly up-regulated expression ($P < 0.05$). Genes are color coded as in C. Data were obtained in two independent experiments measuring biological quadruplicates of each genotype.

Sylamer analysis using all 7-nt motifs complementary to seed regions of mouse miRNAs revealed a highly significant ($P < 8 \times 10^{-13}$; Bonferroni corrected $< 7 \times 10^{-10}$) enrichment for the 7-nt seed match of miR-451 (AACGGTT) in the 3′ UTRs of genes in a cohort of 588 genes, most of which were up-regulated in miR144/451$^{-/-}$ erythroid precursors (Fig. 4 B). Enrichment of the seed sequence of miR-144 (ATACTGT) was observed, but was less significant ($P < 4 \times 10^{-6}$, Bonferroni corrected $< 4 \times 10^{-3}$). Genes with 6-nt seed matches for miR-144 were far less affected than those containing miR-451 sites (Fig. 4 C). However, genes containing 6-nt seed matches for both miR-144 and miR-451 displayed a slight additive effect and were more deregulated than genes with miR-451 seed matches alone. The deregulation of a representative panel of the Sylamer-identified miR-144/451 seed-containing genes was validated by quantitative RT-PCR (qRT-PCR; Fig. 4 D). Of the 588 up-regulated genes identified by Sylamer analysis in the miR-144/451$^{-/-}$ erythroblasts, 98 had one or more 6-nt seed matches for miR-451, 226 had seed matches for miR-144, and 57 of these contained seed matches for both (Table S1). Many of these genes have reported roles in terminal erythropoiesis (Table S1), but the majority are loci whose precise expression are only now linked to normal erythroid development (Table S1). This analysis is not suggestive of a single, or few critical miR-144 or miR-451 targets, but rather that the miR-144/451 locus regulates many genes whose collective deregulation derails normal terminal erythropoiesis. We did not find evidence of lineage-inappropriate gene expression, excluding the possibility that the miR-144/451 cluster functions to maintain lineage identity. Together, these data suggest that the miR-144/451 locus functions as a tuner of gene expression, analogous to the function of miR-223 in neutrophils (Baek et al., 2008).

MiR-451 regulates terminal erythropoiesis

Many of our observations suggest that within the miR-144/451 cluster, miR-451 is likely to play the pivotal role in terminal erythropoiesis. First, it displays a far higher expression level than miR-144. Second, our bioinformatics analyses showed a greater statistical enrichment for the miR-451 seed in the up-regulated cohort of genes in the miR-144/451 mutants. Third, miR-451 exerted a greater impact on the level of target gene expression than miR-144. To explore the possibility that miR-451 plays a key role in regulating terminal erythropoiesis, we generated and analyzed miR-451–null (mir-451$^{-/-}$) mice (Fig. S1 C). The phenotype of miR-451$^{-/-}$ mice was largely indistinguishable from that of miR-144/451$^{-/-}$ mice (Fig. 5, A–D). Together, these results indicate that deregulation of miR-451 targets is sufficient to impair erythroid development.

In this study, we show that miR-451 expression is strictly dependent on Ago2 function. Indeed, while this manuscript was under review it was shown that biogenesis of miR-451 is thus far unique in that it is Dicer independent but requires the endonuclease activity of Ago2 (Cheloufi et al., 2010; Cifuentes et al., 2010). The phenotype of miR-144/451$^{-/-}$ and miR-451$^{-/-}$ mice is milder than that of Ago2$^{-/-}$ mice (O'Carroll et al., 2007), indicating that additional miRNA loci regulate terminal erythropoiesis. In addition, the viability of miR-451$^{-/-}$ mice suggests that the perinatal lethality in homozygous

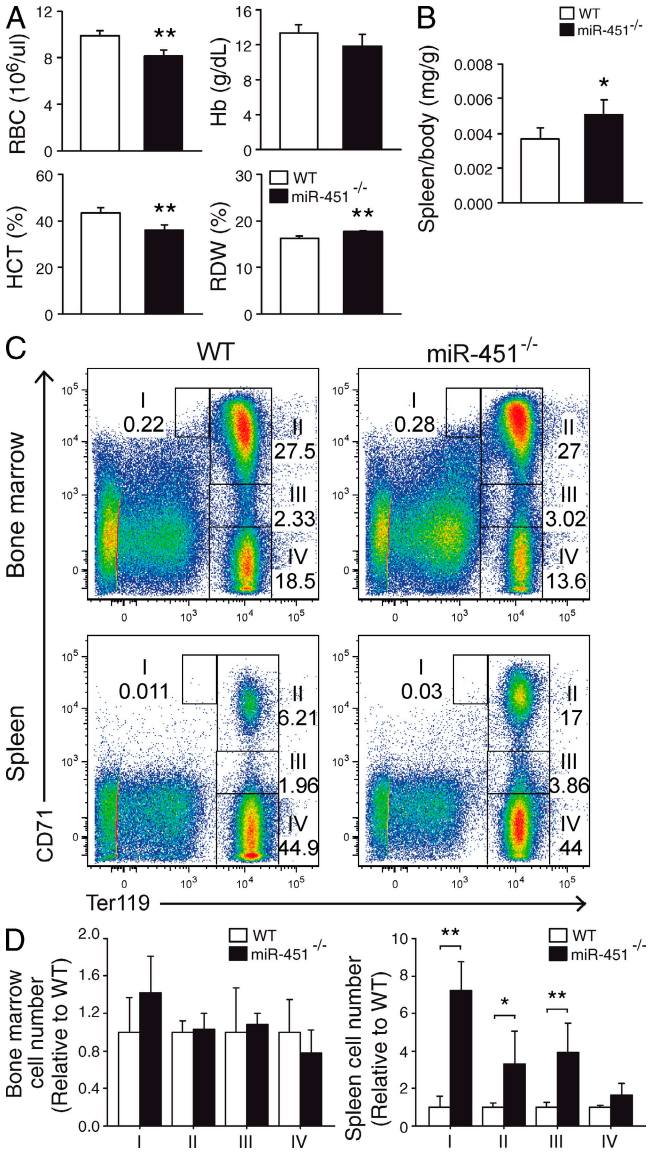

Figure 5. Selective disruption of miR-451 within the miR-144/451 locus results in erythroid hyperplasia, ineffective erythropoiesis, and anemia. (A) MiR-451 deficiency alters several erythrocyte parameters in the peripheral blood. Bar charts are shown expressing values for red blood cell (RBC) numbers, hemoglobin (Hb), hematocrit (HCT); and red cell distribution width (RDW). Bars represent mean values ($n = 4$), error bars indicate standard deviation. (B) Splenomegaly in miR-451$^{-/-}$ mice. Bars represent mean values ($n = 4$), error bars indicate standard deviation. (C) Representative FACS analysis of erythroid cell populations in the bone marrow and spleen of wild-type and miR-451$^{-/-}$ mice. (D) Comparative enumeration of erythroid precursors in the bone marrow and spleen of miR-451$^{-/-}$ and wild-type mice. For B and C, data are represented as in Fig. 2. *, $P < 0.05$; **, $P < 0.01$. The data in all panels are from biological quadruplicates and representative of two independent experiments.

endonuclease-dead *Ago2*^{ADH} mutant mice cannot be accounted for solely by the loss of miR-451 expression. Analogous to the granulocytic and the lymphoid lineages, we now show that a miRNA-encoding locus regulates erythroid development in vivo. We demonstrate that loss of miR-144/451 or miR-451 does not block any one process, but renders terminal erythroid differentiation inefficient. We show that the miR-144/451 cluster tunes the expression of many genes. Gata1 confers the erythroid lineage-specific expression of miR-144/451 (Dore et al., 2008). Therefore, Gata1 not only ignites the program of terminal erythroid differentiation, but also ensures that gene expression is tuned through the activation of the miR-144/451 locus.

MATERIALS AND METHODS

MiRNA expression analysis. RNA was isolated using Trizol (Invitrogen) according to manufacturer's instructions. 500 ng of total RNA was labeled and hybridized to miRCURY LNA microRNA arrays V.11 (Exiqon) for miRNA profiling. Array Express accession no. E-TABM-996. qRT-PCR were performed using TaqMan miRNA assays (Applied Biosystems) for miR-144 and miR-451 and snRNA U6, respectively. In situ hybridizations were performed on cryosections with specific LNA probes (Exiqon).

Generation of miR144/451- and miR-451-null alleles. The MiR-144/451 targeting strategy allows Cre-mediated deletion of transcription start site (TSS) for the miR-144/451 cluster, as well as the hairpin that encodes miR-144. This deletion simultaneously deletes miR-144 and transcription initiation of the cluster, leading to the loss of both miR-144 and miR-451 expression. The *miR-144/451* gene-targeting vector (*pDTA-miR-144/451*) carries a neomycin resistance (*neo*^{r}) gene flanked with two *frt* sites and a *lox*P site (*neo*^{r}*-frt2-lox*P cassette) located *3′* of the TSS and a second *lox*P site between miR-144 and miR-451.

The MiR-451 targeting strategy allows Cre-mediated deletion of the hairpin that encodes miR-451. This deletion leaves the TSS and miR-144 transcription intact, resulting in the loss of miR-451 expression. The *miR-451* gene-targeting vector (*pDTA-miR-451*) carries a *lox*P site between miR-144 and miR-451 and a neomycin resistance (*neo*^{r}) gene flanked with two *frt* sites and a *lox*P site (*neo*^{r}*-frt2-lox*P cassette) located *3′* of the hairpin that encodes miR-451.

The targeting constructs were transfected into IB10 ES cells. Southern blotting of the individual ES cell clones was used to identify homologous recombinants. Targeted ES cells were used to generate mice heterozygous for the *miR-144/451*– and *miR-451*–targeted alleles. These mice were then crossed to the FLP-expressing transgenic mice (FLPeR) to remove the *frt* flanked *neo*^{r} cassette, and then to Del-Cre mice. These genetic manipulations resulted in the generation of *miR-144/451 and miR-451 loxP* alleles, and *miR-144/451* and *miR-451 null* alleles, respectively. All analysis was performed on mice that did not carry the FLPeR or Del-Cre alleles.

All of the mice were bred and maintained in EMBL Mouse Biology Unit, Monterotondo, in accordance with Italian legislation (Art. 9, 27. Jan 1992, n°116) under license from the Italian Ministry of Health.

Analysis of hematopoietic system. Isolation of spleen and bone marrow, and subsequent FACS analysis were performed as previously described (Socolovsky et al., 2001; Pronk et al., 2007). Blood parameters were analyzed using flow cytometry-based hematology (Hemavet HV950FS; Drew Scientific). The analysis of plasma EPO levels were performed using the Quantikine Mouse/Rat immunoassay (R&D Systems).

Histology. Femur and spleen isolated from adult wild-type and miR-144/451$^{-/-}$ mice was fixed in paraformaldehyde and embedded in paraffin. Hematoxylin and eosin (H&E) staining was performed on 8 μm sections. Images were acquired on a microscope (DM6000B; Leica) with 10×, 0.25 numerical aperture dry lens, and 63×, 1.3 numerical aperture oil immersion lens fitted with a DFC290 camera and processed with Adobe Photoshop (Adobe Systems).

Generation of miR-144/451$^{-/-}$ bone marrow chimaeras. Adult mice were sacrificed and bone marrow cells isolated and transferred (2×10^6 cells per recipient) into lethally irradiated (875R) C57BL/6 mice. Bone marrow–reconstituted mice were maintained on medicated water (Baytril; Bayer) for 4 wk after reconstitution and analyzed 3 mo after transfer.

Phenylhydrazine treatment. Adult male mice were administered with phenylhydrazine at a dose of 48 mg/kg by intraperitoneal injection on two successive days, as previously described (Gutiérrez et al., 2008).

Erythroid in vitro culture system. The in vitro expansion and differentiation of erythroid cells from E12.5 fetal livers was performed as previously described (Dolznig et al., 2001; von Lindern et al., 2001). Cell size reduction during differentiation was indirectly assayed by FSC-A using FACS analysis. To assess morphology, cells were spun onto glass slides, air dried, and stained with o-dianisidine (Neutral Benzidine; Sigma-Aldrich) in 1% methanol and Diff Quick staining set (Medion Diagnostics AG). Images were acquired with a microscope at 63×, 1.30 numerical aperture oil immersion lens fitted with a DFC290 camera and processed with Adobe Photoshop. The appearance of nascent reticulocytes was enumerated using a modified FACS protocol as described (Kingsley et al., 2006). Instead of Hoechst 33342, cells were stained for 30 min at 37°C with 20 μM Vybrant Violet (Invitrogen). CFSE labeling and dilution was used to monitor the number of cell divisions upon terminal differentiation as described (Gutiérrez et al., 2008). Annexin V FACS staining (Annexin V apoptosis detection kit; eBioscience) was used to enumerate the number of apoptotic cells in the cultures.

Gene expression data analysis. Live proliferating erythroblasts (FSC-A^{hi}) from eight independent erythroid cultures (four wild-type and four miR-144/451$^{-/-}$) was sorted by FACS to obtain highly homogeneous cell populations for gene expression profiling. Total RNA was isolated using Trizol (Invitrogen) according to the manufacturer's instructions and profiled using Illumina mouse WG-6 v2.0 Bead arrays. Probe level data from all eight arrays were obtained from the Illumina GenomeStudio software and processed using R/BioConductor using a variance stabilizing transformation and robust spline normalization as implemented in the lumi package (Du et al., 2008). Differential expression between wild-type and miR-144/451$^{-/-}$ samples was assessed by fitting linear models and using an empirical Bayes approach to shrink the estimated variance, by means of the limma package (Smyth, 2004). Probe annotations and mappings were obtained from Illumina (MouseWG-6_V2_0_R2_11278593_A). The gene expression data are deposited in Array Express under the accession no. E-MTAB-277.

Quantitative real-time PCR. Total RNA was reverse transcribed by Superscript II reverse transcription (Invitrogen) using random hexamer primers. Quantitative PCR was performed on a LightCycler 480 PCR instrument (Roche) using 2x SYBR green I master (Roche). The expression data were normalized to *Hprt* and *Pgk1* reference genes and analyzed by REST software (Pfaffl et al., 2002) using pairwise fixed reallocation and randomization test to estimate relative normalized fold change between wild-type and miR-144/451$^{-/-}$ erythroblast samples.

Sylamer analysis. The gene-expression data for each probe were sorted according to t-statistic from most significantly up-regulated to most significantly down-regulated in the knockout samples. Each probe ID was mapped to a mouse transcript, and then to a 3′ UTR sequence. The 3′ UTR sequences were obtained by mapping probes to transcript sequences from Vega, Ensembl, or RefSeq, in that order of preference. An ordered list of 19,600 unique transcripts was produced in this fashion, each with a corresponding 3′ UTR sequence. Sylamer was run on this dataset with Markov correction set to filter trinucleotide biases and analyzing enrichment of 7-nt motifs.

Online supplemental material. Fig. S1 illustrates and validates the generation of the miR-144/451 and miR-451 null alleles, respectively. Fig. S2 depicts histological analysis of peripheral blood, BM, and spleen of

miR-144/451–deficient mice, as well as FACS analysis enumerating erythroid precursors. Morphological analysis of in vitro erythroid cultures is also shown. Fig. S3 contains the analysis of lethally irradiated mice reconstituted with miR-144/451$^{-/-}$ bone marrow. Table S1 lists the Sylamer-identified target genes of miR-144/451. Online supplemental material is available at http://www.jem.org/cgi/content/full/jem.20100458/DC1.

We gratefully acknowledge the support E. Perlas and V.Benes of EMBL's Histology and Genecore core facilities, respectively. We also acknowledge the services of Jeanette Rientjes from Monash University's Gene Recombineering Facility.

The authors have no conflicting financial interests.

Submitted: 5 March 2010
Accepted: 13 May 2010

REFERENCES

Baek, D., J. Villén, C. Shin, F.D. Camargo, S.P. Gygi, and D.P. Bartel. 2008. The impact of microRNAs on protein output. *Nature*. 455:64–71. doi:10.1038/nature07242

Bauer, A., F. Tronche, O. Wessely, C. Kellendonk, H.M. Reichardt, P. Steinlein, G. Schütz, and H. Beug. 1999. The glucocorticoid receptor is required for stress erythropoiesis. *Genes Dev*. 13:2996–3002. doi:10.1101/gad.13.22.2996

Broudy, V.C., N.L. Lin, G.V. Priestley, K. Nocka, and N.S. Wolf. 1996. Interaction of stem cell factor and its receptor c-kit mediates lodgment and acute expansion of hematopoietic cells in the murine spleen. *Blood*. 88:75–81.

Bushati, N., and S.M. Cohen. 2007. microRNA functions. *Annu. Rev. Cell Dev. Biol.* 23:175–205. doi:10.1146/annurev.cellbio.23.090506.123406

Cheloufi, S., C.O. Dos Santos, M.M. Chong, and G.J. Hannon. 2010. A dicer-independent miRNA biogenesis pathway that requires Ago catalysis. *Nature*. doi:10.1038/nature09092

Cifuentes, D., H. Xue, D.W. Taylor, H. Patnode, Y. Mishima, S. Cheloufi, E. Ma, S. Mane, G.J. Hannon, N. Lawson, S. Wolfe, and A.J. Giraldez. 2010. A novel miRNA processing pathway independent of dicer requires Argonaute2 catalytic activity. *Science*. doi:11.1126/science.119089

Doench, J.G., and P.A. Sharp. 2004. Specificity of microRNA target selection in translational repression. *Genes Dev*. 18:504–511. doi:10.1101/gad.1184404

Dolznig, H., F. Boulmé, K. Stangl, E.M. Deiner, W. Mikulits, H. Beug, and E.W. Müllner. 2001. Establishment of normal, terminally differentiating mouse erythroid progenitors: molecular characterization by cDNA arrays. *FASEB J.* 15:1442–1444.

Dore, L.C., J.D. Amigo, C.O. Dos Santos, Z. Zhang, X. Gai, J.W. Tobias, D. Yu, A.M. Klein, C. Dorman, W. Wu, et al. 2008. A GATA-1-regulated microRNA locus essential for erythropoiesis. *Proc. Natl. Acad. Sci. USA*. 105:3333–3338. doi:10.1073/pnas.0712312105

Du, P., W.A. Kibbe, and S.M. Lin. 2008. lumi: a pipeline for processing Illumina microarray. *Bioinformatics*. 24:1547–1548. doi:10.1093/bioinformatics/btn224

Du, T.T., Y.F. Fu, M. Dong, L. Wang, H.B. Fan, Y. Chen, Y. Jin, S.J. Chen, Z. Chen, M. Deng, et al. 2009. Experimental validation and complexity of miRNA-mRNA target interaction during zebrafish primitive erythropoiesis. *Biochem. Biophys. Res. Commun*. 381:688–693. doi:10.1016/j.bbrc.2009.02.122

Giraldez, A.J., Y. Mishima, J. Rihel, R.J. Grocock, S. Van Dongen, K. Inoue, A.J. Enright, and A.F. Schier. 2006. Zebrafish MiR-430 promotes deadenylation and clearance of maternal mRNAs. *Science*. 312:75–79. doi:10.1126/science.1122689

Gutiérrez, L., S. Tsukamoto, M. Suzuki, H. Yamamoto-Mukai, M. Yamamoto, S. Philipsen, and K. Ohneda. 2008. Ablation of Gata1 in adult mice results in aplastic crisis, revealing its essential role in steady-state and stress erythropoiesis. *Blood*. 111:4375–4385. doi:10.1182/blood-2007-09-115121

Hammond, S.M., S. Boettcher, A.A. Caudy, R. Kobayashi, and G.J. Hannon. 2001. Argonaute2, a link between genetic and biochemical analyses of RNAi. *Science*. 293:1146–1150. doi:10.1126/science.1064023

Hutvágner, G., and P.D. Zamore. 2002. A microRNA in a multiple-turnover RNAi enzyme complex. *Science*. 297:2056–2060. doi:10.1126/science.1073827

Kingsley, P.D., J. Malik, R.L. Emerson, T.P. Bushnell, K.E. McGrath, L.A. Bloedorn, M. Bulger, and J. Palis. 2006. "Maturational" globin switching in primary primitive erythroid cells. *Blood*. 107:1665–1672. doi:10.1182/blood-2005-08-3097

Lewis, M.A., E. Quint, A.M. Glazier, H. Fuchs, M.H. De Angelis, C. Langford, S. van Dongen, C. Abreu-Goodger, M. Piipari, N. Redshaw, et al. 2009. An ENU-induced mutation of miR-96 associated with progressive hearing loss in mice. *Nat. Genet*. 41:614–618. doi:10.1038/ng.369

Lim, L.P., N.C. Lau, P. Garrett-Engele, A. Grimson, J.M. Schelter, J. Castle, D.P. Bartel, P.S. Linsley, and J.M. Johnson. 2005. Microarray analysis shows that some microRNAs downregulate large numbers of target mRNAs. *Nature*. 433:769–773. doi:10.1038/nature03315

Lu, J., S. Guo, B.L. Ebert, H. Zhang, X. Peng, J. Bosco, J. Pretz, R. Schlanger, J.Y. Wang, R.H. Mak, et al. 2008. MicroRNA-mediated control of cell fate in megakaryocyte-erythrocyte progenitors. *Dev. Cell*. 14:843–853. doi:10.1016/j.devcel.2008.03.012

O'Carroll, D., I. Mecklenbrauker, P.P. Das, A. Santana, U. Koenig, A.J. Enright, E.A. Miska, and A. Tarakhovsky. 2007. A Slicer-independent role for Argonaute 2 in hematopoiesis and the microRNA pathway. *Genes Dev*. 21:1999–2004. doi:10.1101/gad.1565607

Papapetrou, E.P., J.E. Korkola, and M. Sadelain. 2009. A Genetic Strategy for Single and Combinatorial Analysis of miRNA Function in Mammalian Hematopoietic Stem Cells. *Stem Cells*. 28:287–296.

Pase, L., J.E. Layton, W.P. Kloosterman, D. Carradice, P.M. Waterhouse, and G.J. Lieschke. 2009. miR-451 regulates zebrafish erythroid maturation in vivo via its target gata2. *Blood*. 113:1794–1804. doi:10.1182/blood-2008-05-155812

Pfaffl, M.W., G.W. Horgan, and L. Dempfle. 2002. Relative expression software tool (REST) for group-wise comparison and statistical analysis of relative expression results in real-time PCR. *Nucleic Acids Res*. 30:e36. doi:10.1093/nar/30.9.e36

Pronk, C.J., D.J. Rossi, R. Månsson, J.L. Attema, G.L. Norddahl, C.K. Chan, M. Sigvardsson, I.L. Weissman, and D. Bryder. 2007. Elucidation of the phenotypic, functional, and molecular topography of a myeloerythroid progenitor cell hierarchy. *Cell Stem Cell*. 1:428–442. doi:10.1016/j.stem.2007.07.005

Schwenk, F., U. Baron, and K. Rajewsky. 1995. A cre-transgenic mouse strain for the ubiquitous deletion of loxP-flanked gene segments including deletion in germ cells. *Nucleic Acids Res*. 23:5080–5081. doi:10.1093/nar/23.24.5080

Selbach, M., B. Schwanhäusser, N. Thierfelder, Z. Fang, R. Khanin, and N. Rajewsky. 2008. Widespread changes in protein synthesis induced by microRNAs. *Nature*. 455:58–63. doi:10.1038/nature07228

Smyth, G.K. 2004. Linear models and empirical bayes methods for assessing differential expression in microarray experiments. *Stat. Appl. Genet. Mol. Biol.* 3:Article3.

Socolovsky, M., H. Nam, M.D. Fleming, V.H. Haase, C. Brugnara, and H.F. Lodish. 2001. Ineffective erythropoiesis in Stat5a(-/-)5b(-/-) mice due to decreased survival of early erythroblasts. *Blood*. 98:3261–3273. doi:10.1182/blood.V98.12.3261

van Dongen, S., C. Abreu-Goodger, and A.J. Enright. 2008. Detecting microRNA binding and siRNA off-target effects from expression data. *Nat. Methods*. 5:1023–1025. doi:10.1038/nmeth.1267

von Lindern, M., E.M. Deiner, H. Dolznig, M. Parren-Van Amelsvoort, M.J. Hayman, E.W. Mullner, and H. Beug. 2001. Leukemic transformation of normal murine erythroid progenitors: v- and c-ErbB act through signaling pathways activated by the EpoR and c-Kit in stress erythropoiesis. *Oncogene*. 20:3651–3664. doi:10.1038/sj.onc.1204494